

Infrared Frequency Selective Surface Based on Circuit-Analog Square Loop Design

Brian Monacelli, *Student Member, IEEE*, Jonothan B. Pryor, *Member, IEEE*, Ben A. Munk, *Life Fellow, IEEE*, Dale Kotter, and Glenn D. Boreman, *Member, IEEE*

Abstract—A frequency selective surface (FSS) was designed to have a resonant spectral signature in the infrared. The lithographically composed, layered structure of this infrared FSS yields a resonant response in absorption to infrared radiation at a wavelength determined by its FSS element structure and the structure of its substrate layers. The infrared spectral characteristics of this surface are studied via Fourier transform infrared spectroscopy and spectral radiometry in the 3 to 15 μm region of the spectrum. The design is based on circuit-analog resonant behavior of square loop conducting elements.

Index Terms—Frequency selective surfaces (FSS), infrared measurements, infrared radiometry.

I. INTRODUCTION

THE modification of a surface's spectral radiation signature, in absorption, reflection, or transmission, is possible by patterning the surface with conducting elements or with apertures in a conducting sheet. Spectral modifications have been readily shown in the literature for millimeter wave [1]–[5] and infrared [5]–[13] spectral regions and are well known as frequency selective surfaces (FSS). Such surfaces can be configured to function as low-pass, high-pass, bandpass, or dichroic filters [7], [8], [14]–[18]. FSS can even be used as narrowband infrared sources [8], [19], [20] by virtue of Kirchhoff's Law [21], [22] in which the FSS absorptive properties equal its emissive properties. Other applications include FSS use as a pollutant sensing element [23], as a reflecting element in an infrared laser cavity [24] and as an infrared source with a unique emission spectrum.

There are many parameters that affect FSS spectral behavior. Different structures of the conducting elements (or apertures) lead to various resonant characteristics. Also influencing FSS spectral performance is the distribution of the FSS elements and the electrical parameters of the surrounding media. The effects of these fundamental FSS parameters are discussed in the literature [1], [2], [5]. In this paper, we pack conducting square loop

elements into a square grid array. This FSS configuration, in coordination with its stratified substrate, acts as a circuit-analog absorber.

This paper will discuss each step of the square loop FSS composition: its design, fabrication, and characterization. The design was performed using well-known Periodic Method of Moments (PMM) code [25]. A unique aspect of this FSS is its operation in the infrared spectral region. In common FSS design for millimeter waves operation, the FSS can be composed via photoetching of conducting sheets [12], vapor deposition onto photoresist [13], or laser milling. To scale the FSS for infrared operation, it was necessary to fabricate via electron beam lithography (EBL). This technique has been demonstrated [6]–[13], and improvements to these designs are discussed in this writing. The characterization is performed using two different spectral measurement systems for corroboration of the observations.

II. DESIGN

Several techniques to model frequency selective surfaces have been proposed in the literature [26]–[29]; for this research, a robust and widely-used software package was chosen. The FSS design employs code known as the Periodic Method of Moments (PMM) [25]. This code has been used for millimeter wave FSS design [30], [31] and is capable of designing frequency selective surfaces to operate at the higher frequencies of the infrared. The details of this code are discussed in [25]. PMM output plots the reflection and transmission spectra for the electric field and the power spectra of radiation reflected and transmitted by a FSS.

This FSS design has a circuit analog because of the element structure and the substrate layer. Fig. 1 shows a schematic of the designed square loop FSS and its circuit analog, which can be explained as follows: the metal loops give to inductance to the FSS as incident radiation excites current in these wires. Both the 200 nm gaps between the metallic loops and the 1 μm gaps within the loops (to a lesser degree) compose capacitors with a dielectric (air) gap. A resistance is present because this FSS is composed of lossy metallic elements on a dielectric substrate [31], [32]. Thus, an analog RLC circuit network can be envisioned for this geometry.

The square loop configuration is chosen due to its symmetry. This symmetry eases the fabrication tolerances because straight lines reproduce lithographically with higher fidelity and allows the elements to be tightly packed to deter the onset of grating lobes in the spectral response. This FSS is also relatively insensitive to the polarization state of incident radiation when used in absorption due to the square symmetry. When the FSS is caused

Manuscript received February 7, 2004; revised June 1, 2004. This work was supported by the U.S. Department of Energy, Advanced Technology Program, under the DOE Idaho Operations Office Contract DE-AC07-94ID13223.

B. Monacelli and G. D. Boreman are with the College of Optics and Photonics: CREOL & FPCE, University of Central Florida, Orlando, FL 32816-2700 USA (e-mail: Monacelli@CREOL.UCF.edu).

J. B. Pryor was with the ElectroScience Laboratory, The Ohio State University, Columbus, OH 43212-1191 USA. He is now with Harris Corporation, Melbourne, FL 32902 USA.

B. A. Munk is with the ElectroScience Laboratory, The Ohio State University, Columbus, OH 43212-1191 USA.

D. Kotter is with Idaho National Engineering and Environmental Laboratory (INEEL), Idaho Falls, ID 83415 USA.

Digital Object Identifier 10.1109/TAP.2004.841290

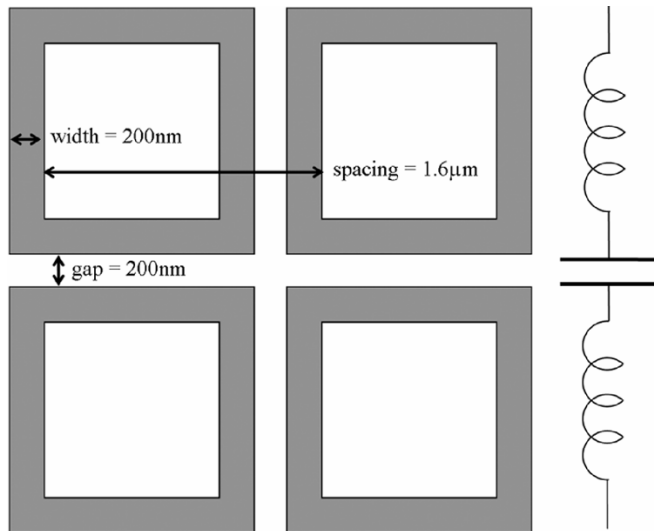


Fig. 1. Schematic of a portion of the repeated FSS and its LC circuit analog. Gray lines represent metal loops, white areas are clear to the substrate. If the FSS metal is lossy, a resistive component also exists in the circuit.

to emit, it is expected to radiate with polarization components along both transverse dimensions of the metallic loop, radiating in neither state preferentially.

Care is taken in selecting the FSS element structure, element material and substrate material. The electrical characteristics of the FSS elements and surrounding media have the effect of shaping and stabilizing the spectral curves with respect to incidence (or emission) angle, as well as the polarization state of the incident radiation. For instance, the presence of a dielectric substrate slightly detunes the FSS resonance and the loop lengths are adjusted to accommodate. Characteristics and influences of the metallic loop and substrate materials are further discussed in Section III. Comparison of modeled spectra to experimental data is shown in Section IV.

III. FABRICATION

A. Process

The square loop FSS was written on a stratified substrate with a JEOL 5900 scanning electron microscope (SEM) converted for EBL, employing Raith ELPHY Quantum pattern generation and overlay software (Leica EBPG 5000+EBL system was later used to fabricate larger FSS). The base of this substrate was composed of a silicon wafer of $375\ \mu\text{m}$ thickness for mechanical stability during fabrication and testing. The active layers consist of the following: a 150 nm gold ground plane was thermally evaporated onto the bare, clean silicon wafer using a BOC Edwards evaporation system. An amorphous silicon standoff layer was then added via radio frequency diode sputtering using a MRC 8667 sputtering system. The thickness of this silicon layer is instrumental to the FSS performance, as will be discussed in the following section.

This substrate was then prepared for EBL by spin-coating a bilayer resist consisting of 200 nm of copolymer poly(methyl methacrylate)/methacrylic acid (MMA(8.5)MAA), topped with 150 nm of 950 k poly(methyl methacrylate) (PMMA). The bilayer with high molecular weight PMMA assists electron beam

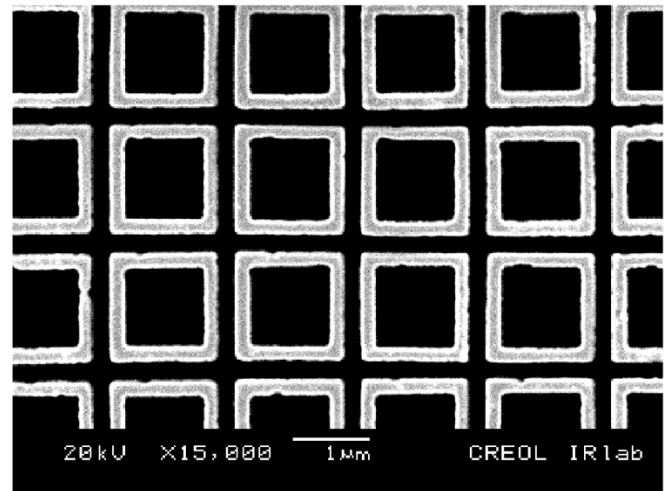


Fig. 2. SEM micrograph of the completed FSS. White lines are the manganese metal loops; black areas are clear to the substrate.

resolution [33]–[35] and improves metal film lift off. Square loop structures were written in this resist at a calibrated line dose of $33\ \text{nC/cm}$. The fine loop line width of 200 nm is shown in Fig. 2, an SEM micrograph of a portion of the functional FSS. This feature size is well within the resolution of the SEM/EBL system, producing a uniform pattern across the field. To fill the minimum sample field requirement of the optical characterization systems, the FSS must extend over a one millimeter square. This was accomplished by stitching $500\ \mu\text{m}$ square write fields in a two by two array. Small stitching errors between write fields, of less than 20 nm, were observed, but their effect on FSS functionality was not quantified.

After exposure in the EBL system, the FSS is developed in a 25% solution of methyl isobutyl ketone in isopropanol (3:1::IPA:MIBK). The device is then taken through a descum process in oxygen plasma to ensure clarity of the written features.

The deposition and feasibility of various metals was characterized. Different metals were studied because the resistivity of the metallic FSS layer is a critical parameter—a lossy metal assists in shaping the FSS absorption spectrum. All metals were deposited via thermal evaporation; features were lifted off in a methylene chloride bath with ultrasonic agitation. The FSS was cleaned with solvents and dried with dry nitrogen before spectral characterization.

B. Discussion of Stratified FSS Composition

The functional FSS consists of the following layered structures: a 150 nm gold ground plane, an amorphous silicon standoff layer and a thin, patterned surface of metallic square loops. The silicon wafer is purely used as a rigid, stable structure. The ground plane renders the base wafer electrically and optically irrelevant because radiation will not pass this optically thick ground plane; infrared radiation is significantly attenuated in 150 nm of gold. This layer not only can be viewed as an electrical ground plane, but as a reflector that will reradiate infrared radiation that is incident upon it.

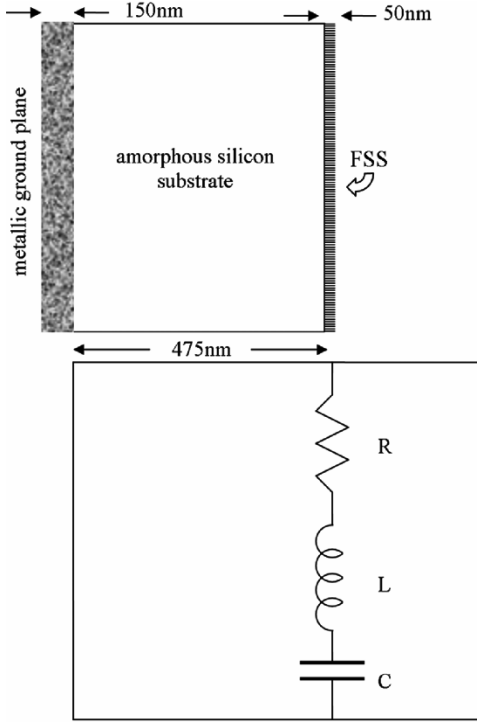


Fig. 3. Cross-section of the FSS strata and its RLC circuit analog and its quarter-wave transmission line to the ground plane.

Therefore, the amorphous silicon layer is included as isolation from this ground plane and it is tuned such that the thickness of this layer is approximately one-quarter wave at the design wavelength of resonance at $6.5 \mu\text{m}$. That is

$$d_{\text{quarter-wave}} = \frac{\lambda}{4n} \quad (1)$$

where $n = 3.42$, the refractive index of the amorphous silicon layer. This 475 nm *a*-Si layer acts as an optical resonant cavity to enhance the performance of the metallic loop FSS. In the circuit-analog theory, this layer can be considered a quarter wave transmission line. A cross-section of the fabricated FSS and its circuit analog is shown in Fig. 3.

When composing the FSS design as a circuit-analog absorber, it is critical to know the electrical characteristics of the lossy (absorbing) FSS metallic layer [1], [31]. Thus, the dc resistivity of readily available metals was characterized via four-point probe. It is assumed that dc resistivity values of metal films scale uniformly to infrared frequency resistivity values, such that a material with a high dc resistivity will have a high resistivity at infrared frequencies. Since thin film resistivity scales indirectly with film thickness, a high resistivity metal is desired so that the FSS layer may be as thick and uniform as possible, such that uniform metallic grains are allowed to grow during deposition. Twenty-five nanometer thin films of chromium and nickel were compared to a 50 nm thin film of manganese. Manganese, a particularly high-resistivity metal [36], was selected such that the thickest possible high resistivity metallic layer was realized to yield the lossy sheet resistance value of approximately $100 \text{ ohms per square}$.

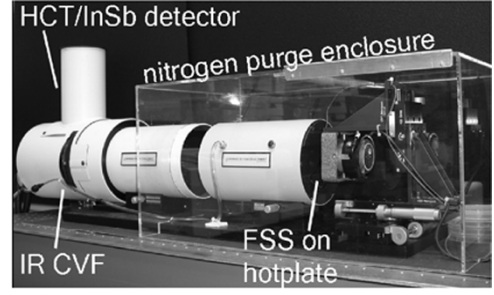


Fig. 4. Image of the spectral radiometer, including the nitrogen purge enclosure, hotplate and alignment stage used for FSS characterization.

IV. CHARACTERIZATION AND RESULTS

A. Measurement of IR FSS Radiance and Emissivity

Two spectral measurement systems were used to study the square loop FSS, a Perkin-Elmer Spectrum One™ Fourier transform infrared (FTIR) micro-spectrometer and an infrared spectral radiometer, manufactured by Infrared Systems Development Corporation of Orlando, Florida.

The FTIR micro-spectrometer is employed to study the reflection characteristics of the FSS. Given zero transmission through the FSS, the device absorption will be one minus the measured reflection. The FTIR system is used in conjunction with a microscope with a $100 \mu\text{m}$ aperture. This small aperture enables fabrication of a small prototype FSS, which is important because the serial nature of electron beam lithography leads to long write times. Using this system, a $100 \mu\text{m}$ square field of FSS elements can be quickly and repeatedly written and tested. The FTIR system was operated in a nitrogen gas purge environment to mitigate the absorption effects of atmospheric carbon dioxide and water. After initial verification of performance, a larger FSS was fabricated to enable further testing and macroscopic demonstration.

The spectral radiometer was used in an imaging configuration in which a 1 mm^2 image field was filled by the FSS. This system is shown in Fig. 4. It was also operated in a nitrogen gas purge enclosure to eliminate the absorption effects of atmospheric carbon dioxide and water. This system is designed to collect energy emitted from the sample under test and measure the resulting spectral signal using a continuous variable filter that scans from 3 to $14.5 \mu\text{m}$. The radiometer is equipped with two detectors to cover this spectral region, a mercury cadmium telluride (MCT) detector for long-wave detection and an indium antimonide (InSb) detector for shorter wavelengths. This system is calibrated with a blackbody source at $200 \text{ }^\circ\text{C}$. After a calibration data are obtained, the raw output voltage of this system is converted to radiance, with dimensions of watts per square centimeter per steradian. All subsequent measurements are converted to radiance data using these blackbody calibration data.

The ratio of the FSS radiance, M_{FSS} , to blackbody radiance, M_{bb} , when measured *at the same temperature* is known as the sample's emissivity

$$\epsilon(\lambda) = \frac{M_{\text{FSS}}(\lambda)}{M_{\text{bb}}(\lambda)}. \quad (2)$$

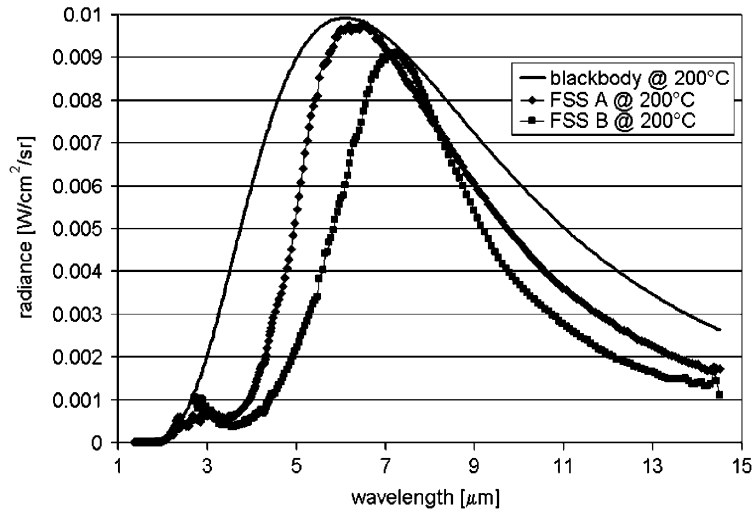


Fig. 5. Radiance of a blackbody and both FSS structures at 200 °C.

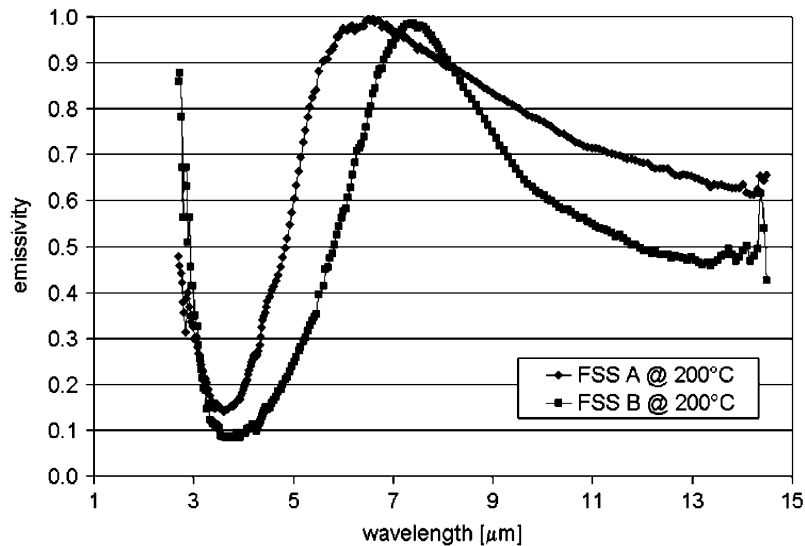


Fig. 6. Emissivity spectra of both FSS structures at 200 °C.

A plot of the spectral emissivity illustrates the ability of the FSS to resonate, shifting radiance out of certain spectral bands and contouring the surface emission. Fig. 5 compares the measured radiance of a blackbody to the radiance spectra of the two surfaces studied. The blackbody and both surfaces were studied at the same elevated temperature of 200 °C.

B. Effect of FSS Substrate Parameters

To demonstrate the ability to control the FSS resonant wavelength, two frequency selective surface structures were investigated. Their difference is the thickness of the *a*-Si standoff layer. FSS *A* has a standoff layer thickness of 475 nm and gives an emission resonance at a wavelength of 6.5 μm. FSS *B* has standoff thickness of 540 nm and resonates at 7.36 μm. The emissivities of these surfaces are compared in Fig. 6. The data of this figure are calculated using (2). Both surfaces give excellent emission contrast between the 3 to 5 μm band and the 5 to 8 μm band, and reasonable contrast when comparing the 8 to 12 μm band to the 5 to 8 μm band. Maximum contrast is

nearly 90% between emission measurements near 4 μm and at resonance. Also, note that the shape of the emission spectrum is comparable for both surfaces, because their metal loop FSS element structures are identical.

C. Comparison of Measured Performance to PMM Modeling

To illustrate the validity of the modeling software, Figs. 7 and 8 compare the results of the PMM modeling to the experimental data for FSS *A* and FSS *B*, respectively. Deviations between the model and experiment could stem from shortcomings in the modeling, such as the inability to implement a spectral dielectric function for the FSS materials. Also accountable for differences in these plots are nonideal lithographic artifacts, such as stitching errors between write fields or broken metallic loops that appear intermittently on the lithographically composed FSS.

Data output by the PMM model may be compared to the emissivity data as shown in Figs. 7 and 8 because the FSS are designed such that all radiation will be emitted or reflected. The

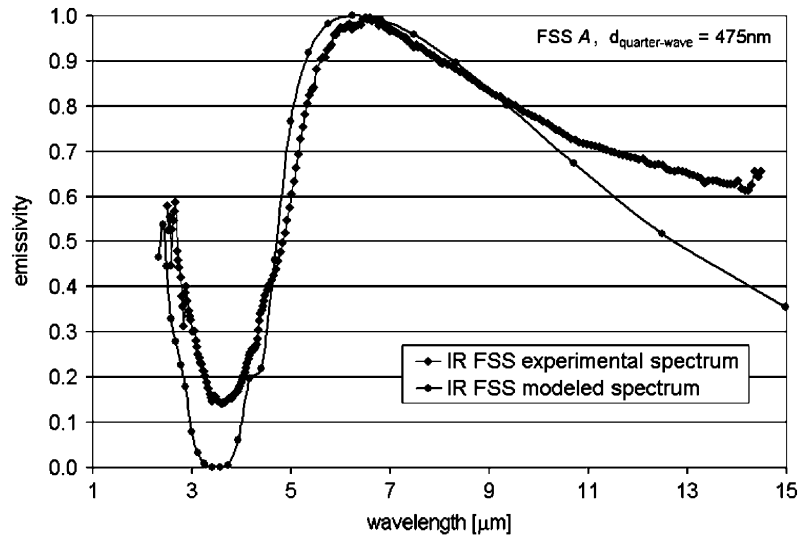


Fig. 7. Modeled performance compared to experimental data for FSS *A*, with a standoff layer thickness of 475 nm.

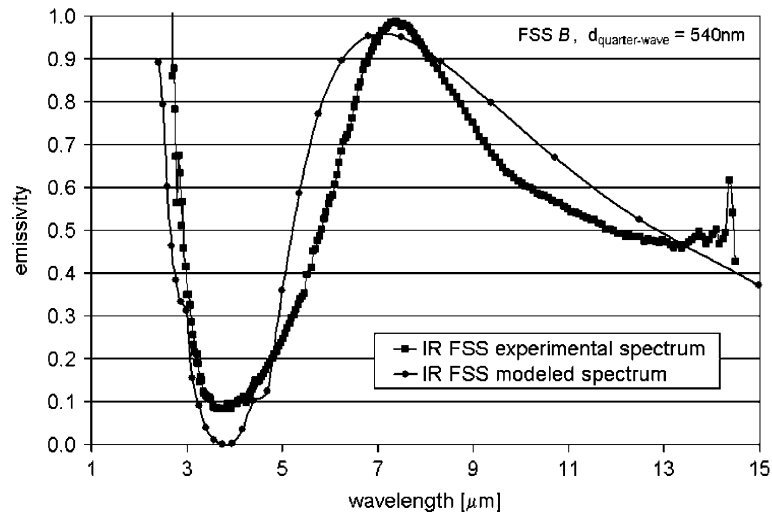


Fig. 8. Modeled performance compared to experimental data for FSS *B*, with a standoff layer thickness of 540 nm.

ground plane allows for zero transmission of infrared radiation. PMM output gives the reflected signal expected from the FSS, such that one minus this reflection spectrum is the spectral signal emitted from the FSS.

D. Influence of Superstrate on IR FSS Performance

It is desired to shape the resonate behavior of this infrared signature to more abruptly cut off the emissivity at longer wavelengths in order for the FSS to behave as a symmetric wavelength bandpass filter. An attempt was made to alter this signature as such by means of a transparent superstrate. In millimeter applications of FSS, it has been shown [1], [4] that the addition of a superstrate layer narrows the FSS spectral response and decreases sensitivity of the spectral response to operational angle. Furthermore, successful application of a superstrate layer can allow for the addition of cascaded FSS layers, which also have the effect of contouring the spectral signature.

This study involved the deposition of a silicon dioxide layer atop the fabricated FSS. The thickness of this layer is

one-quarter wave at resonance; a circuit analog to this layer is to more closely impedance match the composite FSS impedance to that of free space. Measurements of the FSS with the SiO₂ overcoat are shown in Fig. 9. It remains apparent that the FSS has a resonance near 6.5 μm . However, other interesting, albeit undesirable, features appear. The primary resonance is greatly reduced and shifted to a slightly longer wavelength. A second resonance is evident at 9.9 μm ; this resonance corresponds to material absorption of silicon dioxide [37]. Due to this material phenomenon, a narrower FSS spectral signature is not evident, but these findings support the potential to use a superstrate to cascade FSS, if a suitable material can be found with a flat absorption spectrum over this wavelength range.

V. CONCLUSION AND FUTURE WORK

In this paper, we pack conducting square loop elements in a tight square grid array in an effort to shape the emission spectrum of the composite frequency selective surface. We demonstrate the robustness of the PMM modeling as it is used in a new

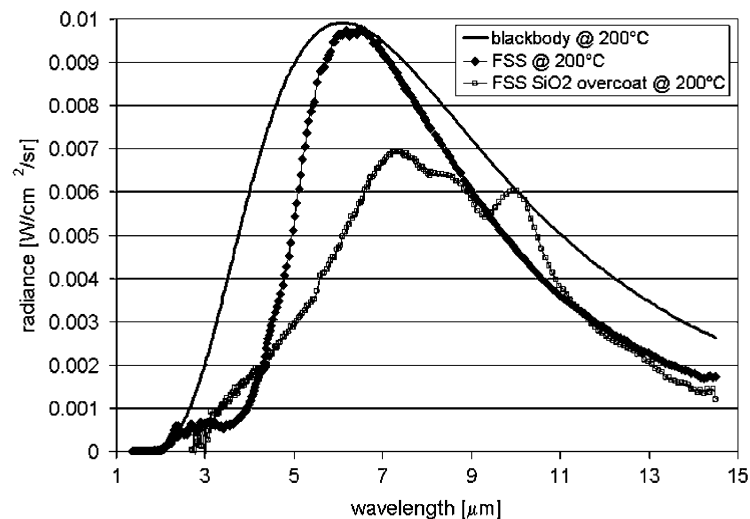


Fig. 9. Comparison of blackbody radiance to FSS radiance with and without SiO_2 superstrate. The addition of a second resonance due to SiO_2 material absorption is detrimental to desired FSS behavior.

frequency regime, for infrared radiation. Agreement between the PMM model and measured data is good for FSS compositions on two different substrates. Nanolithography used to scale the FSS to dimensions necessary for infrared operation proved successful. Results show excellent resonant performance in the infrared, with an emission maximum at wavelengths of $6.5 \mu\text{m}$ and $7.36 \mu\text{m}$. Also, out of band emission is as much as 90% less than emission at resonance.

Alternative element structures, element distributions and substrate or superstrate media are being examined in ongoing work. A method of shaping the FSS resonance response to that of a symmetrical bandpass filter by decreasing long wavelength emission is to incorporate a second cascaded surface of conducting elements in a similar periodic array, [38], [39], [40]. Materials with high infrared transmission and low, uniform infrared absorption are being researched to act as the standoff layer for such a cascaded FSS.

Another desirable configuration is to fabricate this FSS on a flexible substrate, such as Kapton, rather than on a rigid silicon wafer, so that the FSS can be contoured [41] to the surface on which it is applied. Furthermore, research is presently being conducted in an attempt to realize a FSS device capable of resonant tuning, i.e., a structure with variable electrical properties such that the wavelength of resonance can be shifted [42].

ACKNOWLEDGMENT

The authors would like to thank A. Duran of Infrared Systems Development, Orlando, FL for assistance with their radiometric measurements. Also, H. Hockel of the College of Optics and Photonics at the University of Central Florida and I. Young, M. Butler and E. Tapley of Leica Microsystems Lithography, Cambridge, U.K. assisted with electron beam lithography of the IR FSS.

REFERENCES

- [1] B. A. Munk, *Frequency Selective Surfaces: Theory and Design*. New York: Wiley, 2000, pp. 2–23.
- [2] T. K. Wu, *Frequency Selective Surface and Grid Array*. New York: Wiley, 1995.
- [3] T. W. Leonard and L. R. Young, "Frequency selective surfaces," in *Proc. IEEE Antennas Propag. Symp.*, vol. 15, Jun. 1977, pp. 560–563.
- [4] R. Pous and D. M. Pozar, "A frequency-selective surface using aperture-coupled microstrip patches," *IEEE Trans. Antennas Propag.*, vol. 39, no. 12, pp. 1763–1769, Dec. 1991.
- [5] R. Mittra, C. H. Tsao, and W. L. Ko, "Frequency selective surfaces with applications in microwaves and optics," in *Proc. IEEE Microwave Symp.*, vol. 80, May 1980, pp. 447–449.
- [6] I. Puscasu, W. L. Schaich, and G. Boreman, "Modeling parameters for the spectral behavior of infrared frequency-selective surfaces," *Appl. Opt.*, vol. 40, no. 1, pp. 118–124, 2001.
- [7] I. Puscasu, D. Spencer, and G. Boreman, "Refractive-index and element-spacing effects on the spectral behavior of infrared frequency-selective surfaces," *Appl. Opt.*, vol. 39, no. 10, pp. 1570–1574, 2000.
- [8] I. Puscasu, W. L. Schaich, and G. Boreman, "Resonant enhancement of emission and absorption using frequency selective surfaces in the infrared," *Infrared Phys. Technol.*, vol. 43, pp. 101–107, 2002.
- [9] W. L. Schaich, G. Schider, J. R. Krenn, A. Leitner, F. R. Aussenegg, I. Puscasu, B. Monacelli, and G. Boreman, "Optical resonances in periodic surface arrays of metallic patches," *Appl. Opt.*, vol. 42, no. 28, pp. 5714–5721, 2003.
- [10] G. Schider, J. R. Krenn, A. Hohenau, H. Ditlbacher, A. Leitner, F. R. Aussenegg, W. L. Schaich, I. Puscasu, B. Monacelli, and G. Boreman, "Plasmon dispersion relation of Au and Ag nanowires," *Phys. Rev. B*, vol. 68, no. 15, p. 155427, 2003.
- [11] T. Schimert, M. E. Koch, and C. H. Chan, "Analysis of scattering from frequency-selective surfaces in the infrared," *J. Opt. Soc. Amer. A*, vol. 15, pp. 1545–1553, 1990.
- [12] F. Baumann, W. A. Bailey Jr., A. Naweed, W. D. Goodhue, and A. J. Gatesman, "Wet-etch optimization of free-standing terahertz frequency-selective structures," *Opt. Lett.*, vol. 28, no. 11, pp. 938–940, Jun. 2003.
- [13] K. E. Paul, C. Zhu, J. C. Love, and G. M. Whitesides, "Fabrication of mid-infrared frequency-selective surfaces by soft lithography," *Appl. Opt.*, vol. 40, no. 25, pp. 4557–4561, Sep. 2001.
- [14] K. D. Möller, J. B. Warren, J. B. Heaney, and C. Kotecki, "Cross-shaped bandpass filters for the near- and mid-infrared wavelength regions," *Appl. Opt.*, vol. 35, no. 31, pp. 6210–6215, Nov. 1996.
- [15] C. M. Rhoads, E. K. Damon, and B. A. Munk, "Mid-infrared filters using conducting elements," *Appl. Opt.*, vol. 21, no. 15, pp. 2814–2816, Aug. 1982.
- [16] C. Winnewisser, F. Lewen, J. Weinzierl, and H. Helm, "Transmission features of frequency-selective components in the far infrared determined by terahertz time-domain spectroscopy," *Appl. Opt.*, vol. 38, no. 18, pp. 3961–3967, Jun. 1999.
- [17] S. T. Chase and R. D. Joseph, "Resonant array bandpass filters for the far infrared," *Appl. Opt.*, vol. 22, no. 11, pp. 1775–1779, Jun. 1983.

- [18] D. M. Byrne, A. J. Brouns, F. C. Case, R. C. Tiberio, B. L. Whitehead, and E. D. Wolf, "Infrared mesh filters fabricated by electron beam lithography," *J. Vac. Sci. Technol. B*, vol. 3, no. 1, pp. 268–271, Jan./Feb. 1985.
- [19] S. O. C. Giraud and D. G. Hasko, "Mesoscale thermal infrared sources," *Microelec. Eng.*, vol. 41/42, pp. 579–582, 1998.
- [20] J. LeGall, M. Olivier, and J. J. Greffet, "Experimental and theoretical study of reflection and coherent thermal emission by a SiC grating supporting a surface-phonon polariton," *Phys. Rev. B*, vol. 55, no. 15, pp. 10 105–10 114, 1997.
- [21] W. L. Wolfe, *Introduction to Radiometry*. Bellingham, WA: SPIE Press, 1998, vol. TT29.
- [22] E. Dereniak and G. Boreman, *Infrared Detectors and Systems*. New York: Wiley, 1996.
- [23] J. Meléndez, A. J. de Castro, F. López, and J. Meneses, "Spectrally selective gas cell for electro-optical infrared compact multigas sensor," *Sens. Actuators A*, vol. 46–47, pp. 417–421, 1995.
- [24] R. Ulrich, T. J. Bridges, and M. A. Pollack, "Variable metal mesh coupler for far infrared lasers," *Appl. Opt.*, vol. 9, no. 11, pp. 2511–2516, Nov. 1970.
- [25] L. W. Henderson, "Introduction to PMM, Version 4.0," The Ohio State Univ., ElectroScience Lab., Columbus, OH, Tech. Rep. 725 347-1, Contract SC-SP18-91-0001, Jul. 1993.
- [26] R. J. Luebbers and B. A. Munk, "Analysis of thick rectangular waveguide windows with finite conductivity," *IEEE Trans. Microwave Theory Tech.*, vol. MTT-21, no. 7, pp. 461–468, Jul. 1973.
- [27] H. Liu and R. Paknys, "Scattering from periodic array of grounded parallel strips, TE incidence," *IEEE Trans. Antennas Propag.*, vol. 50, no. 6, pp. 798–806, Jun. 2002.
- [28] K. D. Möller, O. Sternberg, H. Grebel, and K. P. Stewart, "Inductive cross-shaped metal meshes and dielectrics," *Appl. Opt.*, vol. 41, no. 19, pp. 3919–3926, Jul. 2002.
- [29] J. A. Reed and D. M. Byrne, "Frequency-selective surfaces with multiple apertures within a periodic cell," *J. Opt. Soc. Amer. A*, vol. 15, no. 3, pp. 660–668, Mar. 1998.
- [30] B. A. Munk, D. S. Janning, J. B. Pryor, and D. J. Marhefka, "Scattering from surface waves on finite FSS," *IEEE Trans. Antennas Propag.*, vol. 49, no. 12, pp. 1782–1793, Dec. 2001.
- [31] J. E. Reynolds, B. A. Munk, J. B. Pryor, and R. J. Marhefka, "Ohmic loss in frequency-selective surfaces," *J. App. Phys.*, vol. 93, no. 9, pp. 5346–5358, May 2003.
- [32] M. A. Ordal, L. L. Long, R. J. Bell, S. E. Bell, R. R. Bell, R. W. Alexander Jr., and C. A. Ward, "Optical properties of the metals Al, Co, Cu, Au, Fe, Pb, Ni, Pd, Pt, Ag, Ti, and W in the infrared and far infrared," *Appl. Opt.*, vol. 22, no. 7, pp. 1099–1120, Apr/ 1983.
- [33] E. A. Dobisz, S. L. Brandow, R. Bass, and J. Mitterender, "Effects of molecular properties on nanolithography in polymethyl methacrylate," *J. Vac. Sci. Technol. B*, vol. 18, no. 1, pp. 107–111, Jan./Feb. 2000.
- [34] M. Khoury and D. K. Ferry, "Effect of molecular weight on poly(methyl methacrylate) resolution," *J. Vac. Sci. Technol. B*, vol. 14, no. 1, pp. 75–79, Jan./Feb. 1996.
- [35] D. G. Hasko, S. Yasin, and A. Mumtaz, "Influence of developer and development conditions on the behavior of high molecular weight electron beam resists," *J. Vac. Sci. Technol. B*, vol. 18, no. 6, pp. 3441–3444, Nov./Dec. 2000.
- [36] L. J. Coffey, D. Neely, M. Harman, R. Allott, N. Prior, D. Shepherd, M. Waite, J. S. Wark, D. Chambers, and J. Hawreliak, "Manganese Adhesion Vacuum Deposition Trials," 1999/2000. *Central Laser Facility Annual Report*, Chilton, Didcot, Oxon.
- [37] *Handbook of Optical Constants of Solids*, vol. I, Academic Press, San Diego, CA, 1997. Edward Palik.
- [38] B. A. Munk, R. J. Luebbers, and R. D. Fulton, "Transmission through a two-layer array of loaded slots," *IEEE Trans. Antennas Propag.*, vol. AP-22, no. 6, pp. 804–807, Nov. 1974.
- [39] D. S. Janning and B. A. Munk, "Wave guidance between pairs of periodic surfaces," *IEEE Trans. Antennas Propag.*, vol. 44, no. 8, pp. 336–340, Aug. 2002.
- [40] R. Mittra, C. H. Chan, and T. Cwik, "Analyzing frequency selective surfaces," in *Proc. IEEE*, vol. 76, Dec. 1998, pp. 1593–1615.
- [41] B. Philips, E. A. Parker, and R. J. Langley, "Influence of a curved FSS on the radiation patterns of an enclosed source," in *Proc. IEEE Antennas Propag. Symp.*, Apr. 19, 1996, pp. 524–527.
- [42] C. Mias, "Waveguide and free-space demonstration of tunable frequency selective surface," *Elec. Lett.*, vol. 39, no. 11, pp. 850–852, May 2003.



Brian Monacelli (S'01) received the B.S. degree in applied optics from Rose-Hulman Institute of Technology, Terre Haute, IN, in 2000 and the M.S. degree in optics from the Institute of Optics, University of Rochester, Rochester, NY, in 2001. He is working toward the Ph.D. degree in the College of Optics and Photonics: CREOL & FPCE, University of Central Florida, Orlando.

He has worked as a Research Scientist with Rockedyne Boeing Lasers and (Electro-Optics Systems Division), Silicon Valley Group (Lithography Division) and NSWC-Crane. He is currently a Graduate Research and Teaching Assistant at the College of Optics and Photonics: CREOL & FPCE, University of Central Florida. His research interests include infrared frequency selective surfaces, uncooled antenna-coupled infrared detectors and infrared system design.

Mr. Monacelli is a Student Member of the Optical Society of America (OSA) and the International Society for Optical Engineers (SPIE), Bellingham, WA. He currently serves as President of the CREOL Association of Optics Students and the UCF Student Chapter of the OSA.



Jonathan B. Pryor (M'99) was born in Huntsville, AL, in 1972. He received the B.S. degree in electrical engineering and physics from Southern Methodist University, Dallas, TX, in 1994 and the M.S. and Ph.D. degrees in electrical engineering from The Ohio State University (OSU), Columbus, in 2000 and 2003, respectively.

From, 1994 to 1998, he was an Electronic Systems Engineer with Diebold, Incorporated, North Canton, OH, where he worked on embedded system design and electromagnetic compatibility issues. While at OSU, he served as both a Distinguished University Fellow and as a Graduate Research Associate with the ElectroScience Laboratory. He is currently employed as an Antenna Engineer with Harris Corporation, Melbourne, FL. His research interests include frequency selective surfaces and antenna arrays of finite extent.



Ben A. Munk (M'61–SM'85–F'89–LF'96) received the M.S. degree in electrical engineering from the Technical University (Polytechnical Institute) of Denmark and the Ph.D. degree in electrical engineering from The Ohio State University (OSU), Columbus, in 1954 and 1968, respectively.

He joined the ElectroScience Laboratory (ESL), OSU, in 1964 where he is currently a Professor of Electrical Engineering and a Supervisor. Prior to joining ESL, he was a Chief Designer for A/S Nordisk Antenne Fabrik, Denmark, and an Assistant Group Leader in the antenna section of Rohde and Schwarz in Munich, Germany. Later, he was a Research and Development Engineer with the Andrew Corporation, Chicago, IL, and then an Antenna Research Engineer with the Rockwell Corporation, Columbus, OH. He has been a Consultant to several of the major airplane and satellite companies in the U.S. and he sits on a number of government committees. He has been the advisor for more than 75 Ph.D. and M.Sc. students, many of whom have become successful leaders in industry and academia. He is author of *Frequency Selective Surfaces, Theory and Design* (New York: Wiley, 2000). He holds numerous patents, including the Hybrid Radome Patent; and is the inventor of the four legged loaded element, and coinventor of the three-pole element (Pelton).

Dr. Munk received a Special Citation from General Loh, WPAFB in 1981 for his contributions to the U.S. Air Force, and in 1993 he received the George Sinclair Award for "Pioneering Advances in Frequency Selective Surfaces." From 1981 to 1985, he was an IEEE Antenna and Propagation Society Distinguished Lecturer. He received the Best Paper Award from the ESL in 1974, the Best Published Paper Award (with coauthor C. Larson) from the Lockheed Corporation in 1982, and the OSU College of Engineering Research Award in 1984. He is listed in *American Men and Women of Science* (12th edition).



Dale Kotter received the B.S. degree in electrical engineering from Brigham Young University, Provo, UT, in 1981.

He is a Consulting Engineer at the Idaho National Engineering and Environmental Laboratory (INEEL), Idaho Falls. He has worked at the INEEL for 20 years specializing in the R&D of active interrogation/remote monitoring technologies in national security applications. Recent research includes the development of concealed weapons detection systems for the National Institute of Justice. He has

five U.S. patents, and over 20 publications and papers.

Mr. Kotter is the winner of seven George Westinghouse Signature awards. He is a Member of the Armed Forces Communication and Electronics Association and serves on the Utah State Engineering College Advisory Board.



Glenn D. Boreman (M'78) received the B.S. degree in optics from the University of Rochester, Rochester, NY, and the Ph.D. degree in optics from the University of Arizona, Tucson.

Since 1984, he has been on the faculty of the College of Optics and Photonics: CREOL & FPCE, University of Central Florida, Orlando, where he is presently Trustee Chair Professor of Optics. He is co-author of *Infrared Detectors and Systems* (New York: Wiley, 1996), author of *Basic Electro-Optics for Electrical Engineers* (SPIE Press, 1998),

and *Modulation Transfer Function in Optical and Electro-Optical Systems* (Bellingham, WA: SPIE Press, 2001). He was editor of *Infrared Technology 1988–1998* (Bellingham, WA: SPIE Press). He currently serves as the Editor-in-Chief of *Applied Optics*.

Dr. Boreman is a Fellow of the Optical Society of American (OSA) and the International Society for Optical Engineers (SPIE), Bellingham, WA. Along with his students, he received the 1995 Kingslake Medal from SPIE. He is a past member of the SPIE Board of Directors.